Harnessing PFAS Materials for Advanced Electrolyte Applications for Lithium-ion Batteries

Contents

Executive Summary

The rapid growth in the demand for lithium-ion batteries, particularly in automotive and stationary applications, has spurred intensive research efforts to enhance battery performance, safety, and cost-effectiveness. In this context, the focus has turned towards advancing electrolytes, with particular emphasis on the utilization of per-and polyfluorinated alkyl substances (PFAS) as promising electrolyte materials. This executive summary encapsulates the findings and implications of a comprehensive study investigating the impact of PFAS incorporation on battery systems.

This investigation commenced by exploring the introduction of fluorine atoms into electrolyte solvents to modulate their Highest Occupied Molecular Orbital (HOMO) and Lowest Unoccupied Molecular Orbital (LUMO) energy levels. The study's findings revealed that such manipulation leads to an expansion of the theoretical potential window, indicating a positive influence on oxidation resistance and reduction susceptibility. Linear sweep voltammetry experiments further elucidated that trifluoroethylene carbonate (CF_3EC) additive demonstrated enhanced oxidation resistance, thus enhancing battery performance.

The application of PFAS materials was assessed across diverse battery systems, including high-voltage electrolytes, flame-retardant electrolytes, high-concentration electrolytes, lithium-ion batteries, and lithium metal batteries. These materials were found to play a pivotal role in enhancing battery attributes, thereby establishing their significance in advancing emerging battery technologies.

A critical focus was directed towards the use of PFAS materials in silicon-based negative electrodes. The study revealed the potential of fluoroethylene carbonate (FEC) as an effective additive to enhance cycle capacity retention. However, FEC's chemical instability led to significant gas generation, highlighting the need for alternative additives. Intriguingly, 1,1,2,2-tetrafluoroethyl 2,2,3,3-tetrafluoropropyl ether (D2) emerged as a compelling alternative. D2 exhibited favorable physical properties, such as a low boiling point and absence of a flash point, making it an attractive option for electrolyte modification.

Cycle tests conducted on test batteries validated the positive impact of PFAS materials on cycle capacity retention and reduction of internal resistance. Notably, D2 demonstrated superior gas suppression, emphasising its potential in enhancing battery safety.

In conclusion, this study underscores the pivotal role of PFAS materials in elevating battery performance and safety across various battery systems. The findings highlight the significance of PFAS materials as essential components within electrolytes, accentuating their indispensability in driving advancements in battery technology.

Introduction

Lithium-ion batteries are composed of essential components, including a positive electrode, a negative electrode, an electrolyte, and a separator. Notably, the market trajectory is poised for substantial growth, particularly in sectors such as automotive and stationary batteries. To facilitate this expansion, enhancing the performance, safety, and cost-effectiveness of lithium-ion batteries has become imperative, thus driving vigorous research and development endeavors. Within this framework, considerable attention has been directed towards the advancement of electrolytes, with a particular focus on the utilization of perfluorinated alkyl substances (PFAS) as electrolyte materials, offering a promising avenue to significantly elevate battery performance.[1, 2)]

1 Characteristics of fluorinated solvents

The incorporation of electron-withdrawing moieties such as fluorine atoms into prevailing electrolyte solvents offers the prospect of diminishing the Highest Occupied Molecular Orbital (HOMO) energy level and thereby enhancing oxidation resistance. For instance, the introduction of fluorine substituents into ethylene carbonate (EC), propylene carbonate (PC), and ethylmethyl carbonate (EMC) has been demonstrated to prominently lower their respective HOMO energy levels. This is depicted in Figure 1, illustrating the calculated HOMO and Lowest Unoccupied Molecular Orbital (LUMO) energy levels via Gaussian B3LYP/6-31G(d) computations. Evidently, both the HOMO and LUMO energy levels are effectively attenuated, suggesting a plausible enhancement in oxidation resistance following the incorporation of fluorine atoms. Conversely, the concomitant reduction in the LUMO energy level also implies a heightened propensity for reducibility.

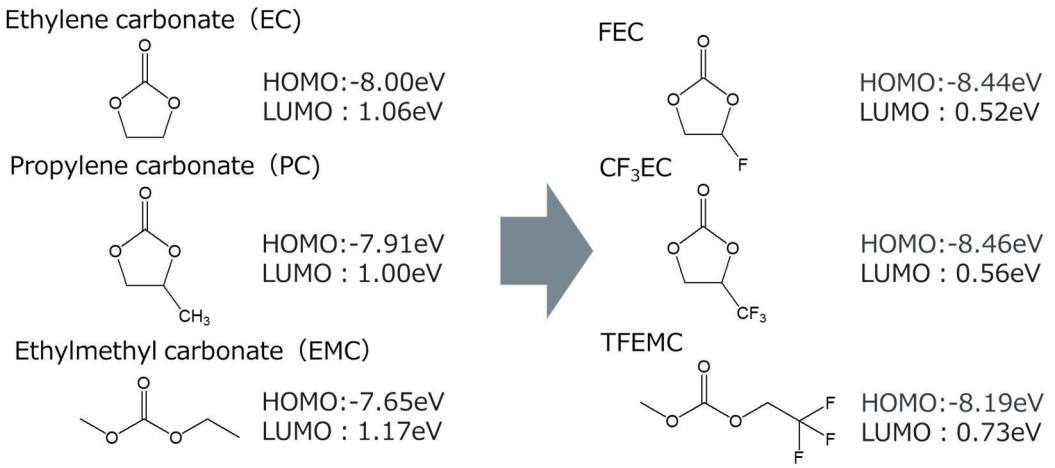

Fig. 1: HOMO and LUMO levels of each compound before and after introduction of fluorine atoms

Figure 2 depicts the outcomes of linear sweep voltammetry conducted across diverse solvents, wherein a platinum (Pt) wire was designated as the working and reference electrode, while an argentum (Ag) wire served as the counter electrode. The electrolyte encompassed $LiPF_6$, dissolved in each solvent to achieve a concentration of 0.1 mol dm^{-3}. Comparative examination of the response current elevation of fluoroethylene carbonate (FEC) and trifluoroethylene carbonate (CF_3EC) with respect to the commonly employed propylene carbonate (PC) solvent reveals a distinctive current surge occurring at a higher potential range for FEC and CF_3EC, indicative of an augmented oxidation resistance. Notably, within FEC, a minor reduction peak manifests around -0.5 V (vs. Ag/Ag^+) on the

reduction axis, implying a possible film formation ensuing from FEC reduction. In contrast, CF_3EC, despite sharing a comparable LUMO energy level, lacks a reduction-induced film formation peak, underscoring its exceptional resistance to reduction. While a correlation between the HOMO energy level and oxidation resistance is evident, the LUMO energy level and reduction resistance may also be influenced by multifaceted solvation environments. Hence, it is plausible that the introduction of fluorine atoms at distinct positions may exert substantial modifications on compound characteristics.

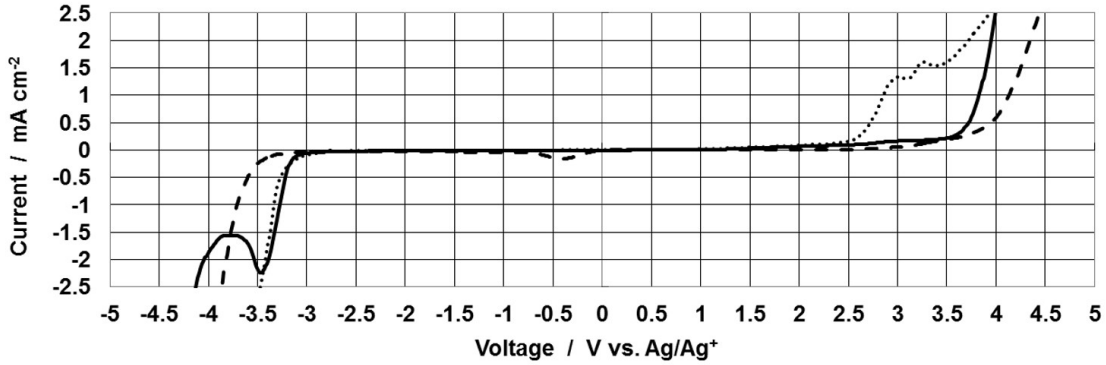

Fig. 2: Relationship between potential and current densities of Pt wire in 0.1mol dm^{-3} $LiPF_6$ PC (⋯), 0.1mol dm^{-3} $LiPF_6$ FEC (- - -) and 0.1mol dm^{-3} $LiPF_6$ CF_3EC (—)

2 Application of PFAS materials in various battery systems

PFAS materials find application in emerging battery technologies, encompassing high-voltage electrolytes[3-7], flame-retardant electrolytes[8-13], high-concentration electrolytes[14-17], lithium-ion batteries[18-20], and lithium metal batteries[21-23], wherein these materials assume a pivotal role.

3 Application of PFAS materials to silicon-based anodes

Silicon-based negative electrodes have emerged as a focal point of investigation for augmenting lithium-ion battery capacity owing to their high theoretical capacity. Nonetheless, the practical utility of silicon-based negative electrodes is constrained by their inherent challenges, including low capacity retention attributed to volumetric expansion during charging and subsequent contraction during discharge, thereby inducing active material cracking and electronic contact deficiency. To ameliorate these limitations, fluoroethylene carbonate (FEC) has garnered attention as an electrolyte additive. In this context, the incorporation of FEC engenders the release of fluorine ions during reduction reactions, leading to the integration of lithium fluoride (LiF) into the solid-electrolyte interphase (SEI) film, thereby bestowing the negative electrode with a stabilised protective

layer. However, a notable concern pertains to FEC's chemical stability, as its propensity for decomposition in the presence of $LiPF_6$ leads to decarboxylation and the evolution of substantial gas volumes. The consequential gas generation exacerbates the challenge of limiting the fill capacity of silicon-based active materials within negative electrodes in practical battery configurations. Consequently, the advancement of gas-suppressing additives for FEC or exploration of alternative compounds assumes a pivotal role in the prospective augmentation of silicon-based active material fill quantities within negative electrodes. As an alternative substance, 1,1,2,2-tetrafluoroethyl 2,2,3,3-tetrafluoropropyl ether (D2) was used for verification.

Table 1 presents the fundamental physicochemical attributes of compound D2. Notably, D2 exhibits a boiling point of 92°C, akin to dimethyl carbonate (DMC), yet its notably depressed melting point prevents facile solidification even under low-temperature conditions. Furthermore, D2 is accompanied by the drawback of elevated viscosity compared to ethylene carbonate (EMC), a hydrocarbon electrolyte solvent. A salient feature of D2 resides in its conspicuous absence of a flash point, thereby obviating any adverse effect on the flash point of the electrolyte upon its inclusion. In line with prevailing observations, fluorine-containing solvents typically precipitate a reduction in both Highest Occupied Molecular Orbital (HOMO) and Lowest Unoccupied Molecular Orbital (LUMO) energy levels, often engendering a shift in the potential window that governs oxidation resistance and reduction susceptibility. Contrarily, D2 prompts a reduction in HOMO levels concomitant with an elevation in LUMO energy levels, thus entailing an expansion of the theoretical potential window. This intriguing phenomenon is speculated to emanate from the interplay between the oxygen bond angle intrinsic to the ether moiety and the electron-withdrawing attributes of fluorine atoms.

Table1: Physical properties of various electrolyte solvent compounds

	Melting point (℃)	Boiling point (℃)	Viscosity @25℃ (mPa·s)	Flash point (℃)	HOMO (eV)*	LUMO (eV)*
D2	-(<-40℃)	92	1.6	No	-9.20	1.20
VC	22	162		72	-6.92	0.01
FEC	17	210		129	-8.44	0.52
EC	36	248	1.9 @40℃	150	-8.00	1.06
EMC	-55	109	0.6	23	-7.65	1.17

*Gaussian09 (B3LYP/6 -31G(d))

The experimental setup encompassed the fabrication of test batteries utilising distinct electrode compositions. Specifically, the positive electrode entailed LiNi0.8Mn0.1Co0.1O2 as the active material, augmented with carbon black as the conductive agent and polyvinylidene fluoride (PVdF) as the binder, formulated in a mass ratio of 92:4:4. Conversely, the negative electrode was formulated employing a composite blend of SiO and artificial graphite in a mass ratio of 10:90 as the active material, complemented by a binder mixture comprising carboxymethyl cellulose and styrene-butadiene rubber in a mass ratio of 97.6:1.2:1.2, while integration with a microporous membrane was effectuated.

A reference electrolyte solution was established by dissolving lithium hexafluorophosphate ($LiPF_6$) within a solvent mixture of ethylene carbonate (EC) and ethyl methyl carbonate (EMC), configured at a volumetric ratio of 3:7, attaining a concentration of 1.0 mol dm^{-3}, wherein the inclusion of vinylene carbonate (VC) was enacted at a weight ratio of 1%. Pertinently, two distinct electrolytic solutions were prepared as the FEC system and D2 system, wherein the former integrated 2% mass of fluoroethylene carbonate (FEC) into the reference electrolyte, and the latter entailed the incorporation of 2% mass of compound D2. Consequentially, single-layer laminate cells were assembled, embedding the synthesised electrodes and electrolyte compositions.

The ensuing cycle tests were conducted at an elevated temperature of 60°C, operating within a voltage range of 2.5-4.2V. Charging was executed in a constant current-constant voltage (CC-CV) mode, with a current rate (CC) set at 1C and a termination condition in CV mode specified as 1/50C. Subsequent discharge was carried out at a rate of 1C. To assess the dynamic characteristics, DC-IR (Direct Current-Internal Resistance) profiles were acquired by subjecting the cell to a discharge procedure at 1C and 10 seconds duration, initiated from a voltage of 3.8V, and performed within a sub-zero environment of -20°C. Figure 3 delineates the correlation between the cycle count and the capacity retention rate, ascertained through the constant current charge/discharge assessments conducted at an elevated temperature of 60°C. Evidently, both the FEC and D2 systems exhibit enhanced capacity retention rates vis-à-vis the reference electrolyte, with the former two systems yielding nearly equivalent capacity retention rates. This convergence implies a comparable contribution of D2 to the formation of a stable solid-electrolyte interphase (SEI) coating akin to FEC, thereby substantiating the potential of D2 to ameliorate cycling performance.

Figure 4 provides an elucidation of the Direct Current-Internal Resistance (DC-IR) resistance values before and post the 60°C cyclic testing regimen. Notably, the FEC and

D2 systems manifest lower initial resistance in contrast to the reference electrolyte, while post-cycling, the D2 system attains the most conspicuous reduction in resistance. Additionally, Figure 5 graphically portrays the evolution of gas generation within the battery during the course of the cycle tests. Noteworthy is the observation that while FEC excels in maintaining cycle capacity retention, it concurrently exhibits the most pronounced gassing. This outcome can be attributed to the relatively diminished chemical stability intrinsic to FEC. In stark contrast, the D2 system markedly curtails gas generation, underscoring its superiority in mitigating battery gas evolution alongside enhancing cycle capacity retention.

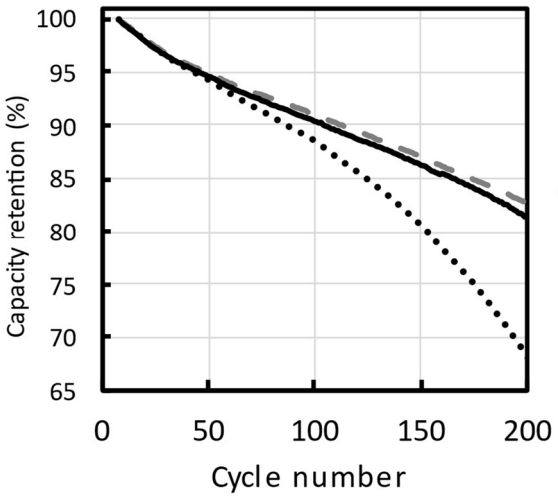

Fig. 3: Capacity retention vs. cycle of cells with REF (…), containing FEC (---), and D2 (—) electrolytes

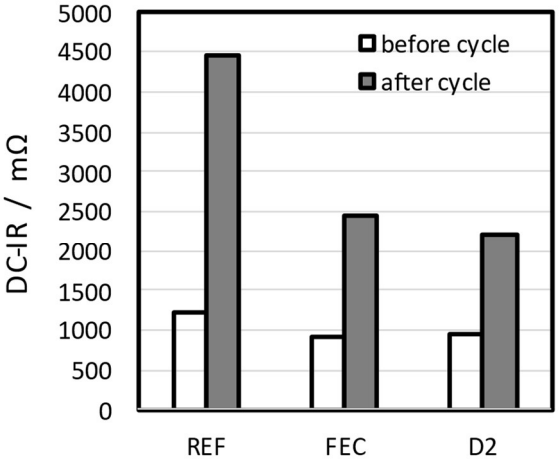

Fig. 4: DC-IR of cells with REF, containing FEC, and D2 electrolytes before and after cycling tests

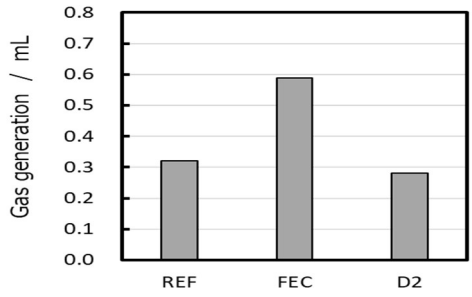

Fig. 5: Gas generation of cells with REF, containing FEC, and D2 electrolytes before and after cycling tests

4 Conclusion

The outcomes of this study unequivocally establish that the incorporation of PFAS materials into electrolytes exerts a substantial positive impact on enhancing both battery performance and safety across diverse battery systems. Consequently, it is evident that PFAS materials assume an essential role as integral constituents within the electrolyte, underscoring their indispensability in the pursuit of advancing battery technology.

5 References

1) N. von Aspern, G.-V. Rçschenthaler, M. Winter, and I. Cekic-Laskovic, “Fluorine and Lithium: Ideal Partners for High-Performance Rechargeable Battery Electrolytes “, Angew. Chem. Int. Ed., 58, 15978-16000, (2019).
2) M. He, C.-C. Su, C. Peebles, and Z. Zhang, Energy Environ. Sci., 6, 1806-1810 (2013).
3) Z. Zhanga, L. Hua, H. Wua, W. Wenga, M. Koh, P. C. Redfernb, L. A. Curtissb, and K. Amine, Energy Environ. Sci., 6, 1806-1810 (2013).
4) T. Kitagawa, K. Azuma, M. Koh, A. Yamauchi, M. Kagawa, H. Sakata, H. Miyawaki, A. Nakazono, H. Arima, M. Yamagata, and M. Ishikawa, Electrochemistry, 78, (2010).
5) L. Xia, S. Lee, Y. Jiang, S. Li, Z. Liu, L. Yu, D. Hu, S. Wang, Y. Liu, and G.Z. Chen, ChemElectroChem,6 (14), 3747 (2019).
6) Z. Wang, S. Zhuang, M. Lu, J. Solid State Electrochemistry, 25, 1353 (2021).
7) W. Hou, D. Zhu, S. Ma, W. Yang, H. Yan, and Y. Dai, J. Power Sources, 517,1 (2022).
8) T. Achiha, T. Nakajima, Y. Ohzawa, M. Koh, A. Yamauchi, M. Kagawa, and H. Aoyama, Journal of The Electrochemical Society, 156 6 A483-A488 2009.
9) T. Achiha, T. Nakajima, Y. Ohzawa, M. Koh, A. Yamauchi, M. Kagawa, and H. Aoyama, Journal of The Electrochemical Society, 157 6 A707-A712 2010.
10) J. Hou, L. Wang, X. Feng, J. Terada, L. Lu, S. Yamazaki, A. Su, Y. Kuwajima, Y. Chen, T. Hidaka, Z. He, H. Wang, and M. Ouyang, Energy Environ. Mater, 6, e12297 (2023).
11) A. Pan, Z. Wang, F. Zhang, L. Wang, J. Xu, J. Zheng, J. Hu, C. Zhao, and X. Wu, Nano Research, 1, (2022).
12) D. Guan, G. Hu, Z. Peng, Y. Cao, J. Wu, M. Huang, S. Zhang, Y. Dai, Y. Gong, and K. Du, J. Materials Chemistry A, 10 (23), 12575, (2022).
13) P. Shi, S. Fang, J. Huang, D. Luo, L. Yang, and S. Hirano, J. Materials Chemistry A, 5 (37), 19982 (2017).
14) M. Haruta, Y. Masuo, T. Moriyasu, A. Tomita, C. Sakakibara, A. Kamei, M. Hirota, T. Takenaka, T. Doi, M. Inaba, Electrochemistry, 2015, 83(10), 837-839
15) T. Doi, Y. Shimizu, M. Hashinokuchi,and M. Inaba, Journal of the Electrochemical

Society. 2017, 164(1), A6412-A6416
16) K. Takada, Y. Yamada, and A. Yamada, ACS Appl. Mater. Interfaces, 11, 35770.35776(2019).
17) A. Bouibes, S. Saha, and M. Nagaoka, Nature research, 10, 21966 (2020).
18) N. Azimi, W. Weng, C. Takoudis, ZC. Zhang, Electrochemistry Communication, 37, 96-99, (2013).
19) K. Dokko, N. Tachikawa, K. Yamauchi, M. Tsuchiya, A. Yamasaki, E. Takashima, J. W. Park, N. Serizawa, and M. Watanabe, J. Electrochem. Soc. 160 (8) A1304 (2013)
20) J. W. Park, K. Yamauchi, E. Takashima, N. Tachikawa, K. Ueno, K. Dokko, and M. Watanabe, J. Phys. Chem. C, 117, 9 4431 (2013).
21) L. Suoa,W. Xueb, M. Gobetd, S. G. Greenbaumd, C. Wang, Y. Chenb, W. Yange,Y. Lie, and J. Lib, PNAS, 115 (6) 1156-1161, 2018.
22) Y. Lee, T. Lee, S. Kim, J. Lee, Y. Ahn, K. Kim, H. Ma, G. Park, S. Lee, S. Kwak, and N. Choi, Nano Energy, 67 104309, (2020).
23) S. Ko, T. Obukata, T. Shimada, N. Takenaka, M. Nakayama, A. Yamada, and Y. Yamada, Nature Energy, 7, 1217 (2022).